Hot Hydrogen Testing of Uranium Nitride Cermet for Nuclear Thermal Propulsion

Benjamin Larson[1,2], Jhonathan Rosales[1], Brian Taylor[1], Jason Reynolds[1], Nathan Jerred[3], Jamelle Williams[1], Arne Croell[4], Martin Volz[1]

[1]*NASA Marshall Space Flight Center, Huntsville, AL 35808*
[2]*Ira A. Fulton College of Engineering and Technology, Brigham Young University, Provo UT 84602*
[3]*Idaho National Laboratory, Idaho Falls, ID 83401*
[4]*RSESC, University of Alabama in Huntsville, 301 Sparkman Dr., Huntsville, AL, 35899*

phone: (385)-251-9573 email: bl277@byu.edu

This study investigated the thermochemical stability and performance characteristics of uranium mononitride tungsten molybdenum cermet (UN-Mo30W) as a potential fuel material for Nuclear Thermal Propulsion (NTP) engines. Twelve monolithic cylinders were subjected to conditions simulating an active NTP engine. The tests demonstrated thermal variability within the test article and highlighted the dissociation of UN into U and N_2 at elevated temperatures, affecting the microstructure and causing bonding between cermet wafers and cooling tubes. Findings indicate that while UN-Mo30W cermet exhibits many desirable properties for NTP service, its practical suitability is limited by high-temperature thermochemical instability.

I. INTRODUCTION

The search for high performance propulsion systems for deep space exploration has led to the investigation of UN-Mo30W cermet as a potential high temperature candidate fuel material for NTP engines. Recent hot hydrogen tests conducted at the Marshall Space Flight Center's Nuclear Thermal Rocket Element Environmental Simulator (NTREES) offer critical insights into the thermochemical stability and performance characteristics of this novel fuel material [1]. NTREES is an experimental test chamber that simulates the temperature, pressure, and hydrogen flow typical of a nuclear thermal engine via induction heating of the test article and injection of various pressurized gases.

This work details the fabrication, testing, and characterization of a high-density cermet material composed of 60 vol.% depleted uranium nitride in a sintered metal-alloy-matrix of 30 wt.% tungsten and 70 wt.% molybdenum. The test article, consisting of twelve individual cylinders, underwent repeated hot hydrogen testing under conditions simulating an active NTP engine including high temperatures, pressures, and exposure to hot hydrogen gas flow.

II. EXPERIMENTAL

The fabrication of the individual segments began with a powder metallurgical approach. The initial powders consisted of depleted uranium mononitride (45-75 µm) supplied by Los Alamos National Laboratory, and a custom alloy, Mo30W, produced by HC Starck with a particle size of approximately 20 µm. The powders were mixed in a powder mixer (Turbula®T2F, W.A. Bachhofen Turbula) to form the cermet mixture to undergo consolidation.

The consolidation was completed via Direct Current Sintering (DCS) with a Thermal Technology DCS-25 unit. DCS produced twelve individual monolithic cylinders 34mm in diameter and 25mm long. The cylinders were machined using wire Electrical Discharge Machining (EDM) at Idaho National Laboratory to facilitate introduction of 37 molybdenum tubes which served both for passages for hydrogen gas and for structural support. Four of the twelve wafers were composed of molybdenum which provided geometric compatibility with pre-existing test equipment while reducing UN feedstock consumption and project expenses related to radiological activities. A custom epoxy resin was used to form a gas-tight seal with the molybdenum tubes at the test article cold end to introduce hydrogen flow during the test. The hot hydrogen exposure involved two 5-minute segments at 2150K and 2550K, respectively. The test conditions are displayed in Table I.

Table I: Test Conditions for Segments 1 and 2

	Segment 1	Segment 2
Chamber Atmosphere	Ar	Ar
Chamber Pressure	6 MPa	6 MPa
Hydrogen Flow	7.93 g/s	6.94 g/s
Peak Temperature	2150K	2550K
Segment Duration	5 min	5 min
Ramp Rate	100 K/min	100 K/min
Peak Power	88.6 kW	115.5 kW

III. RESULTS AND DISCUSSION

III.A. Initial Characterization

A visual inspection was performed after testing and revealed longitudinal surface deformation at cooling channel sites, along with wafer bonding at the area where the maximum temperature was recorded. Figure 1 displays the cermet test article after hot hydrogen exposure.

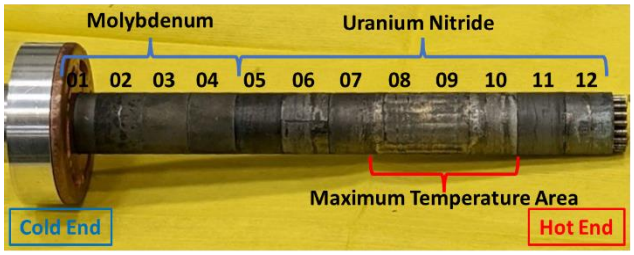

Fig. 1: Test article following hot hydrogen exposure.

Temperature predictions were determined by thermal simulation models employing Finite Element Analysis (FEA) via COMSOL, shown in Figure 2. The models predicted the highest thermal load to be on wafers 8 and 9, which was validated by the characterization results. Surface temperatures during the tests were monitored using a multiwavelength spectropyrometer (FAR FMP2/2X) which measured a maximum surface temperature of 2550 K, consistent with the predicted maximum surface temperature of 2589 K.

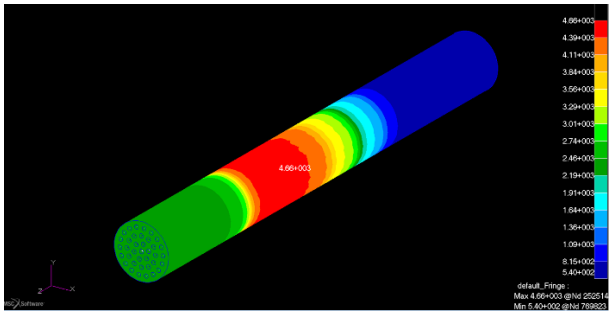

Fig. 2: Predicted thermal distribution during testing.

During disassembly, it was found that several of the outermost molybdenum cooling tubes were unable to be removed due to bonding generated within the cermet wafers. The highest bond concentration was observed among wafers 8, 9, and 10. These three wafers experienced the highest temperature during testing and consequently the highest degree of surface alteration. A structured light scan on the maximum temperature area shows the surface pattern generated during the test, displayed in Figure 3.
Data from the scan indicated a slight preference for valley formation on one side of the test article which could be a result of an uneven thermal distribution. The data was superimposed on an ideal cylinder with a diameter of 33.85mm, showing a maximum deviation of +0.327mm and a minimum of -0.634mm. Pre-test measurements of the wafer sections gave an average diameter of 34.0mm, indicating an overall reduction in average diameter of 0.15mm which is likely attributable to dissociation of UN to uranium metal followed by thermal gradient induced migration to the cooling channel void space.

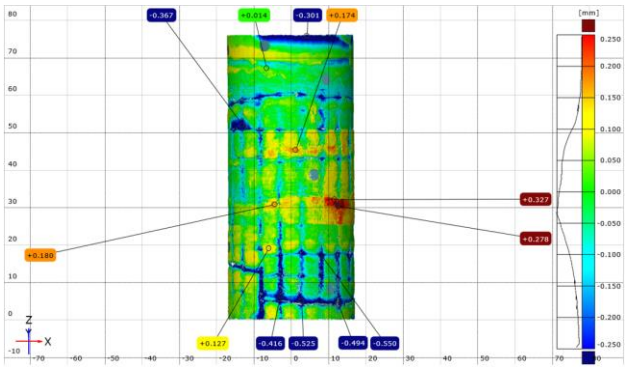

Fig. 3: Structured light scanning data of the test article after testing.

III.B. Microstructural Evaluation

Disassembly was followed by sectioning of areas of interest and examination via optical microscopy and SEM. Figure 4 displays the cross section of wafer 9 showing external cracking, surface deformation, tube bonding on the outermost orifices, and a gradual change in porosity from the center to the periphery. A radial increase in reflectivity of the wafer due to porosity was visually apparent after polishing and was confirmed by the pixel intensity measurements acquired via digital image analysis, displayed in Figure 5.

Fig. 4: Optical micrograph of wafer 9 axial cross-section

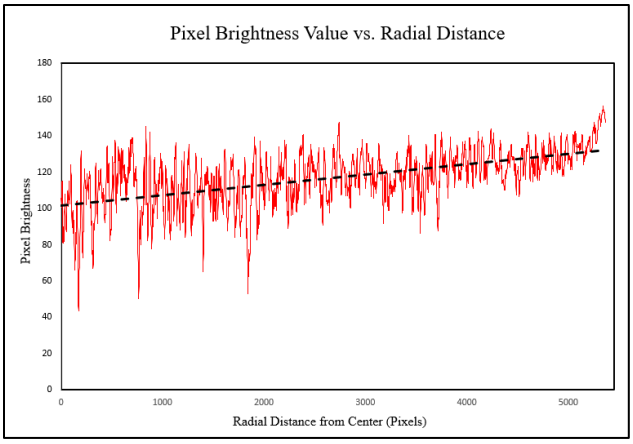

Fig. 5: Pixel brightness values demonstrate increasing reflectivity with increasing radial distance.

In the wafer centers, there were no significant changes in the grain size between the control and tested wafers, including those positioned in the maximum temperature area during the test. However, the edge of wafers from the maximum temperature area demonstrated a notable decrease in porosity in areas composed of UN as displayed in Figure 6a. The microstructure of the central region displayed porosity (Figure 6b) and is consistent with the control wafer. The porosity reduction is attributed to a densification process that may have occurred during testing, as such areas experienced temperatures higher than those employed during the wafer fabrication via DCS.

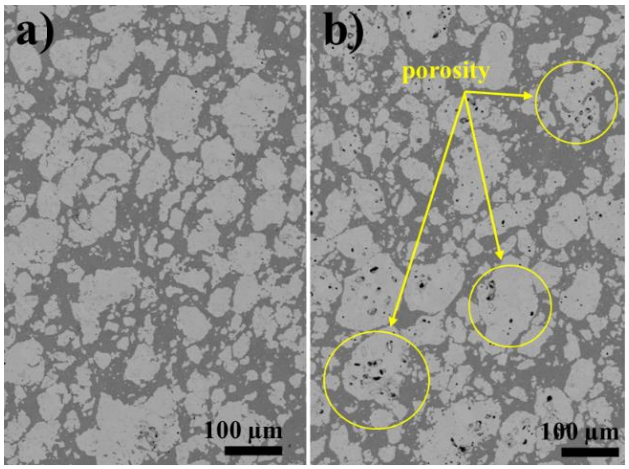

Fig. 6: a) SEM micrograph displaying reduced porosity on the edge region of wafer 9. b) SEM micrograph of center region of wafer 9.

Porosity quantification was performed using image threshold analysis on various areas of interest using the SEM backscatter images and the resulting values were averaged. Porosity values of wafers outside of the maximum temperature area were unchanged from the control, giving an average porosity value of 0.42% ± 0.03%. Conversely, a similar analysis of images taken near the edge of wafers from the maximum temperature area resulted in an average porosity value of 0.06% ± 0.04%. This reduction in porosity was found only near the outer edge of wafers 8, 9, and 10. A heat transfer FEA model displayed in Figure 7 predicted a shallow heat dissipation region for the inductive heating method employed during the test which is consistent with the areas where reduced porosity is observed.

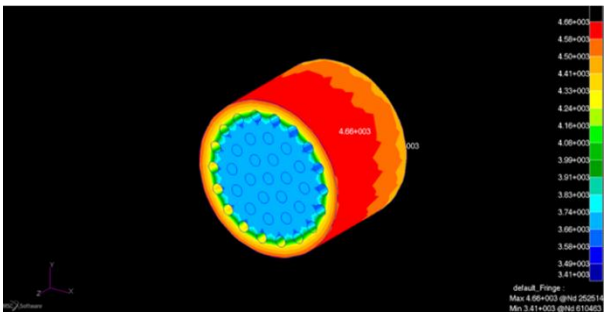
Fig. 7: Predicted cross-sectional thermal distribution.

The main mechanism affecting the microstructure can be attributed to dissociation of UN into U and N_2, which is well documented and typically occurs at or above 1800 ºC [2-4]. This could enable formation of low-melting U-Mo alloys with reduced thermomechanical strength [5,6]. UN dissociation followed by uranium metal migration occurred on the perimeter near the cooling tubes of all wafer sections, leading to bonding between the wafer and tubes in several sections. Previous work from Kuznietz et. al showed that molten uranium can diffuse through W grain boundaries at temperatures below 1,300 ºC [7] and can also dissolve Mo at or below 1160 ºC [8]. A similar mechanism of uranium diffusion and/or dissolution through refractory metal is proposed to occur with the molten uranium and molybdenum cooling tubes. Figure 8 displays a partially bonded molybdenum cooling tube along with melting of the wafer orifice next to the tube.

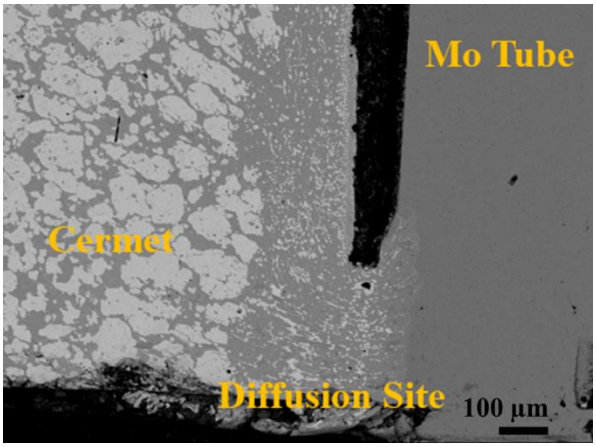

Fig. 8: SEM micrograph displaying bonding between cermet wafer and molybdenum tube.

The diffusion of uranium through the grain boundaries of the refractory metal matrix can be observed in Figure 9, where EDS mapping shows complete phase separation between the Mo30W alloy and the uranium. The smooth edges, reduced particle size, and presence on grain boundaries confirms that a liquid phase of uranium metal diffused through the refractory metal matrix ultimately resulting in a macroscopic change of the cermet fuel wafers.

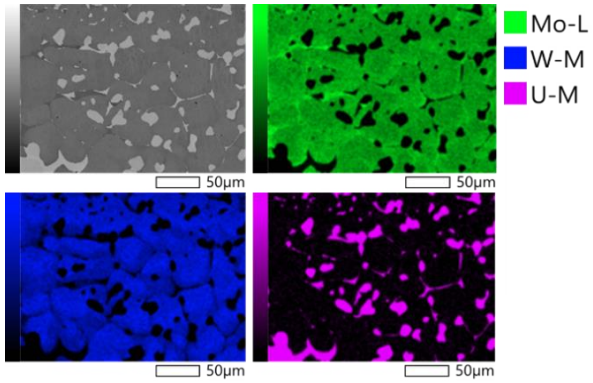

Fig. 9: Electron Dispersive X-Ray Spectroscopy of matrix.

IV. X-Ray Diffraction Analysis

XRD was performed on several samples on areas of interest upon completion of the test, and a summary of the results is shown in Figure 10. The areas of interest include the center, intermediate area, and surface of wafers at several points along the length of the article. The predominant phases observed in all scans were UN and a molybdenum-tungsten mixture. Metallic uranium (γ-U) which is a byproduct of UN dissociation, was observed at the surface of several wafers, primarily those exposed to the highest heat loads during the test. UO_2 was also confirmed by diffraction analyses and its presence is attributed to the UN fabrication process as the precursor material was uranium oxide fuel.

	Sample Wafer ID												
Phase	Control	8	9	10	11	12	7	8	9	10	11	12	Control
γ-U							•	•	•	•	•		
UN	•	•	•	•	•	•	•	•	•	•	•	•	•
UN_2							•	•	•	•	•	•	
UC_2											•		
UO_2	•	•	•	•	•	•	•	•	•	•	•	•	•
MoW	•	•	•	•	•	•	•	•	•	•	•	•	•
MoN												•	
Mo_2C				•	•	•	•			•	•	•	•
MoB										•	•	•	
Mo_2B		•	•	•							•		
BN													•
Graphite											•	•	•

Surface Edge Center

Figure10: Phases confirmed by X-ray diffraction.

Multiple carbide phases including UC_2 and Mo_2C were also reported, and their presence is attributed to the interaction between the Cermet powder and the graphite tooling during the densification process via DCS. Boron constituents including MoB, Mo_2B, and BN were also reported, and their presence is due to the introduction of BN spray during the sintering process. BN coatings were employed in densification via DCS as a releasing agent.

V. CONCLUSION

A nuclear fuel test article composed of a cermet mixture of 60 vol.% UN and 40 vol.% Mo30W alloy matrix was fabricated via DCS and exposed to elevated temperatures under flowing hydrogen in two 5-minute segments, at 2150K and 2550K, respectively. During the tests, the inductive heating method resulted in considerable thermal variability between the center and the outer surface of the test article which is evidenced by the differences in measured properties between these two areas, including difference in density, porosity, and crystallographic structure. This was accurately predicted by thermal simulation models validated in previous work [9].

The characterization results revealed the different mechanisms that affected the composition and structural integrity of the test article. Dissociation of the UN phase was observed in thermally affected areas with dissociation rate positively correlated to temperature, confirming previous experimental results of UN thermochemical stability. Additionally, the molybdenum-based matrix when exposed to liquid uranium leads to the formation of low melting point U-Mo alloys. Also, liquid uranium, a byproduct of UN dissociation, diffused through the intergranular boundaries of the refractory metal matrix and drastically affected the overall structure and properties of the initial cermet material. It was found that diffusion of carbon and boron surface contamination into the cermet material is accelerated at increased temperatures.

Overall, this test confirmed that the UN-Mo30W cermet may not be suitable as a fuel material at the temperatures proposed for a nuclear thermal engine. However, other applications requiring lower operating temperatures may consider the proposed concept. Overall, data collected during this test will be valuable in designing future experiments.

ACKNOWLEDGMENTS

This work was completed at NASA - Marshall Space Flight Center (MSFC) and funded by NASA's Space Technology Mission Directorate (STMD) through the Space Nuclear Propulsion (SNP) project. The NASA Pathways Internship Program in conjunction with the Materials and Processes Laboratory at NASA MSFC supported personnel and facilities to execute all tasks presented. The authors thank the support from the Materials Science Division (MST-8) at Los Alamos National Laboratory for fabricating the UN fuel feedstock.

Portions of this research were completed in collaboration with The University of Alabama in Huntsville (UAH), supported by NASA MSFC under cooperative agreements NNM11AA01A and 80MSFC22M0004. Special thanks go to my mentor, Dr. Jhonathan Rosales, for his continual advisement and support throughout the duration of this project.

REFERENCES

1. J. ROSALES, “Characterization Report: Hot Hydrogen Test of NTREES-3 Nuclear Fuel Article,” Tech. rep., NASA Marshall Space Flight Center (2019).
2. W.M. OLSON, R.N.R. MULFORD, “The Decomposition Pressure and Melting Point of Uranium Mononitride,” J. Phys. Chem., 67, 952 (1963); https://doi.org/10.1021/j100798a525
3. V. VENUGOPAL et al., “Vapour Pressures of Uranium and Uranium Nitride over UN(s),” J. Nucl. Mat., 186, 259 (1992); https://doi.org/10.1016/0022-3115(92)90345-L
4. V. G. BARANOV et al., “Thermal Stability Investigation Technique for Uranium Nitride,” Ann. Nucl. Energy, 87, 784 (2016). https://doi.org/10.1016/j.anucene.2014.09.023
5. H. OKAMOTO, “U-Mo (Uranium-Molybdenum),” J. Phase Equilib. Diffus., 33, 497 (2012); https://doi.org/10.1007/s11669-012-0095-z
6. T.R.G. KUTTY et al., “Thermophysical Properties of U_2Mo Intermetallic,” J. Nucl. Mat., 420, 193 (2012); https://doi.org/10.1016/j.jnucmat.2011.10.002
7. M. KUZNIETZ et al., “Effect of Liquid Uranium on Tungsten Foils up to 1350°C,” J. Nucl. Mat., 160, 69 (1988); https://doi.org/10.1016/0022-3115(88)90009-8
8. M. KUZNIETZ et al., "Progressive dissolution of molybdenum foils in liquid uranium at 1160° C." J. Nucl Mat. 160, no. 2-3 (1988): 196-200. https://doi.org/10.1016/0022-3115(88)90048-7
9. J. HIRSCHHORN, F. HILTY, M. R. TONKS, and J. ROSALES, “Review and Preliminary Investigation into Fuel Loss from Cermets Composed of Uranium Nitride and a Molybdenum-Tungsten Alloy for Nuclear Thermal Propulsion Using Mesoscale Simulations,” *JOM*, 73, *11*, 3528–3543 (Sep. 2021).